Formation of the retinotectal projection requires Esrom, an ortholog of PAM (protein associated with Myc)

Jasmine D'Souza[1], Michael Hendricks[1], Sylvie Le Guyader[1], Sivan Subburaju[1], Barbara Grunewald[2], Klaus Scholich[3] and Suresh Jesuthasan[1,*]

[1]Developmental Neurobiology Group, Temasek Life Sciences Laboratory, 1 Research Link, Singapore 117604, Rep. of Singapore
[2]Max Planck Institute for Developmental Biology, Spemannstrasse 35, 72076 Tübingen, Germany
[3]Pharmazentrum Frankfurt, Klinikum der Johann Wolfgang Goethe-Universität Frankfurt, 60590 Frankfurt, Germany
*Author for correspondence (e-mail: suresh@tll.org.sg)

Accepted 29 October 2004

Development 132, 247-256
Published by The Company of Biologists 2005
doi:10.1242/dev.01578

Summary

Visual system development is dependent on correct interpretation of cues that direct growth cone migration and axon branching. Mutations in the zebrafish *esrom* gene disrupt bundling and targeting of retinal axons, and also cause ectopic arborization. By positional cloning, we establish that *esrom* encodes a very large protein orthologous to PAM (protein associated with Myc)/Highwire/RPM-1. Unlike motoneurons in *Drosophila highwire* mutants, retinal axons in *esrom* mutants do not arborize excessively, indicating that Esrom has different functions in the vertebrate visual system. We show here that Esrom has E3 ligase activity and modulates the amount of phosphorylated Tuberin, a tumor suppressor, in growth cones. These data identify a mediator of signal transduction in retinal growth cones, which is required for topographic map formation.

Key words: Retinotectal projection, Topographic mapping, Fasciculation, Axon branching, Visual system, Zebrafish

Introduction

For an animal to see well, retinal axons from the eye must innervate their targets in the brain in a well-ordered manner during embryonic development. In vertebrates, the majority of retinal axons project to the optic tectum (or superior colliculus in mammals). An important feature of the retinotectal projection is topographic mapping: the connection of neighboring points in one structure (the retina in this case) to neighboring points in another (the optic tectum). One aspect of topographic mapping that has gained much attention in recent years is the involvement of gradients. Based on the results of surgical manipulations, Sperry proposed that positional information both in the eye and the tectum is provided by graded chemical tags (Sperry, 1963). With the cloning of Eph receptors and ligands in the 1990s, the existence of such gradients was confirmed (Orike and Pini, 1996). Currently, with knockout and misexpression experiments, there is strong evidence that retinal axons use these gradients to determine direction of growth and branching position (Yates et al., 2001; Hindges et al., 2002; Mann et al., 2002; Sakurai et al., 2002).

There are a number of complexities in the establishment of the retinotectal projection that remain poorly understood. Axons that grow to the posterior tectum encounter large changes in the absolute concentration of graded cues, but are still able to interpret small differences across the width of the growth cone. How is this possible? In chemotaxing bacteria, adaptation to changes in absolute concentration involves cyclical desensitization and resensitization to the cue. Growth cones also are capable of this behavior (Ming et al., 2002). Desensitization may occur via ubiquitin-mediated protein degradation, while resensitization requires localized protein synthesis (Campbell and Holt, 2001); the molecular details of this process remain unclear. Other questions revolve around how a retinal growth cone is able to arborize at the correct location. In the zebrafish, axons grow to their target position without branching. They then stop and arborize. There must be some mechanism that correlates positional information in retinal axons with gradient information present on the tectum to produce a change in cellular behavior.

In an effort to better understand the processes involved, a large-scale genetic screen has been carried out in the zebrafish (Baier et al., 1996). One mutant with aberrant topographic mapping isolated in this screen is *esrom* (Karlstrom et al., 1996; Trowe et al., 1996). We report here the positional cloning of *esrom*, and analysis of its function in retinal axons. It has previously been suggested that *esrom* could encode a component of the cytoskeleton (Odenthal et al., 1996). We show here that Esrom is a large protein that affects regulation of the tumor suppressor Tuberin. Based on its properties, we propose that Esrom is involved in the interpretation of cues that mediate topographic map formation.

Materials and methods

Zebrafish strains

Mutant lines were maintained using standard procedures. The *Shh:GFP* (Neumann and Nuesslein-Volhard, 2000) line was crossed to *esr*^{te75}.

DiI/DiD labeling

DiI or DiD (Molecular Probes) was dissolved in chloroform, loaded into pulled glass capillaries and injected into specific regions of the eye using a gas pressure injector. The position of injection was confirmed by confocal microscopy of the eye, and only embryos with non-overlapping label were used for further analysis. The retinotectal projection was imaged using confocal microscopy with a 20× water immersion objective; *z* stacks were deconvolved using Auto-Deblur (AutoQuant Imaging).

Eye transplantation

Transplantations were carried out as described previously (Wagle et al., 2004).

Retinal cultures

Two-day-old embryos were genotyped on the basis of their pigmentation phenotype. Retinae were then isolated, fragmented, placed in glass-bottom culture dishes coated with polylysine and laminin, and grown in L15 medium supplemented with BSA and N1 (Sigma) (Wagle et al., 2004). Both mutant and wild-type explants were placed in different regions of the same dish.

To assess fasciculation, cultures were grown for 24 hours at 28°C. Eight clumps from three different cultures were imaged with a 20× phase objective, using a 12-bit Hammamatsu Orca-II camera on a Leica DM-IRBE microscope. Analysis was carried out with MetaMorph (Universal Imaging). Axons were examined at a distance of 50 μm from the periphery of the clump; the region tool was used to create a line at this distance. The number of single axon and bundles intersecting this line was counted manually. Bundles were defined as two or more axons growing together for a distance of at least 25 μm in the vicinity of the position of assessment. An outgrowth was judged to be a single axon when its width was eight units or less, and the change in intensity relative to background was less than 80 units. These parameters were measured with the linescan function. The ratio of bundles to single axons was calculated for each clump, to correct for any bias due to different clump size.

Mapping and positional cloning

esr^{te50}, *esr*^{te75}, and *esr*^{tno7b} heterozygotes in the AB background were crossed to the WIK strain. The resulting progeny were used as parents for self-crossing and generating haploids. DNA from 3-day-old mutant embryos was extracted in 25 μl TE containing 1.8 mg/ml Proteinase K, which was incubated at 55°C for 6 hours. The total volume in each well was made up to 100 μl. From this, 2.5 μl was used as template for 10 μl PCR reactions. SSLP and SSCP polymorphisms were used for fine-mapping, and a total of 1286 meioses were screened. SSCPs were detected as described (Foemzler and Beier, 1999). The PCR product (4 μl) was run on 8% non-denaturing PAGE, which was then developed by silver staining. The zebrafish genomic PAC library created by Chris Amemiya in the pCYPAC6 vector (German Genome Resource Center) was used for the chromosome walk. PCR-based screening of library number 706 with Z6663, fa97c06, fc50b12 and fj33d03 identified six PAC clones. DNA from these clones was isolated using the Qiagen large-construct kit. Insert ends were sequenced using SP6 and T7 primers. These sequences were then used for walking and building a genomic contig spanning *esrom*. Similarly, a zebrafish BAC library from Inctye Genomics (in the pBeloBAc11vector) was also screened by PCR to isolate clones that were not represented in the PAC library. The contig was shotgun sequenced at the Sanger Center.

Primer pairs used for mapping were: Z6663, CATCTTCATTGCCCAGCC (forward) and ATAGGAGCCCATCTGCACAC (reverse); Z7813, AATTCAATTAGGGCCAGGCT (forward) and ATGCGTGAACCATTACTGCA (reverse); fa97c06, AAAAATTTCCGATTCTGTGAAGG (forward) and ACAAATCTCCTACTTCGCCACAC (reverse); fj33d03, AGAGACCGCGCTTAATAAATCA (forward) AATATGCCGATGGCTAAAACC (reverse).

Gene knockdown by morpholino

Morpholino 1 (CACAGGACTCACTGATGATATGAAGG) was targeted to disrupt the splicing of the first exon within the RCC1 domain, while morpholino 2 (TTATTACTTACAGCAGCCATGTCTT) was designed to target the exon at amino acid 4080, which falls between the Myc-type dimerization domain and B-box zinc finger. Splice sites were predicted by comparison to the human genome. A control morpholino (CCTCTTACCTCAGTTACAATTTATA) and the control provided by Gene Tools were also used. Morpholinos were injected into one-cell stage zebrafish wild-type embryos. Three-day old embryos were screened for the xanthophore phenotype of *esrom* and fixed the next day in 4% paraformaldehyde at 4°C overnight. These embryos were mounted in 1.5% low-melting temperature agarose and the anterior eyes were labeled with DiI. For RT-PCR, RNA was extracted from 2.5-day-old embryos and the RT reaction was carried using an oligo dT primer. The cDNA was PCR amplified using a forward primer in the normal transcript and reverse primer designed within the intronic region.

Cloning of *esrom*

RNA was extracted from 2- to 3-day-old wild-type zebrafish embryonic brain. The 5′ end of *esrom* was cloned using gene specific primer GAAGAGGCAGGCGCAGGATAA for RT reaction followed by RACE with the SMART™ RACE cDNA amplification system (BD Biosciences). For cloning 13 kb of *esrom* cDNA, 2 μg of RNA from 2- to 4-day-old wild-type zebrafish embryo was used for reverse transcription reaction with Powerscript (BD Biosciences) and threhalose. The RT product (2 μl) was used for long-distance PCR with the Expand Long PCR template PCR system (Roche). The primers used were TTTCACTTCGGCCAATTGAACGTGGTTGGATCGCCTGCAATCGGG (forward) and GCCCTGGGCTTGAGCTGCAC (reverse).

E3 ligase assay

A 579 bp fragment bearing the RING domain was cloned in-frame with GST in PGEX-4T2 between *Bam*HI and *Not*I. The construct was transformed in BL21 cells. Bacterial culture (50 ml) was induced at 37°C with 1 mM IPTG for 4 hours. The cells were lysed in lysis buffer (50 mM Tris-HCl pH 7.4, 2 mM EDTA, 0.1% Triton X-100, 1 M $MgCl_2$, 0.1 M $MnCl_2$, 0.3 M PMSF). The protein was pulled down from the supernatant using 200 μl of GST sepharose 4B beads (Amersham Pharmacia Biotech). For the E3 ligase assay, 15 μl of the beads was incubated with reaction buffer (20× is: 1 M Tris pH 7.5, 40 mM ATP, 100 mM $MgCl_2$, 40 mM DTT), 200 nM E1, 0.5 μM E2 and 8 μg Ubiquitin. The reaction was incubated at 30°C for 3 hours and then loaded on 6% PAGE. The western was performed using anti-Ubiquitin antibody and ECL detection system.

Antibody specificity

One-hundred 48-hour-old embryos were homogenized and incubated overnight at 4°C in a protein extraction buffer (10 mM Tris pH 7.4, 2% Triton X-100, 1 mM PMSF, 1 mM aproptinin, 1 mM leupeptin, 1 mM trypsin inhibitor) and centrifuged. The pellet was suspended in 150 ml of 2% SDS and run on a 5% SDS PAGE. The proteins were blot transferred onto a PVDF membrane (BioRad) and probed with the C terminus PAM antibody (Guo et al., 1998) and developed using ECL. The C terminus end of *esrom* containing the LDLRA, RING and the zinc finger was cloned in PGEX-4T and purified as above and run on 8% SDS PAGE and the western was carried out using the same PAM antibody.

A second antibody, made to amino acids 4601-4614 of human PAM (Ehnert et al., 2004), was also used for immunofluorescence. Pre-absorption was carried out by incubating the antibody with a peptide (CPAGPKGKQLEGSE) overnight at 4°C, followed by centrifugation at 100,000 ***g*** for 30 minutes.

Zebrafish ESTs corresponding to human *TSC2* (Zon Lab Comparative Genomics, http://www.tchlab.org) and assembly 2 of the

zebrafish genome (http://www.sanger.ac.uk/Projects/D_rerio/) show 100% amino acid conservation over a 15 residue stretch containing the Ser939 Tuberin phosphorylation site (ESTs: zfishC-a2119f08.p1ca, zfishC-a2119f08.p1cz and zfish41364-379d12.q1c) (Sanger sequences: NA21443, NA442 and NA5028).

RNA in situ hybridization

The intra molecular PHR repeat region was cloned into pGEM-T (Promega). In vitro transcribed DIG-labeled sense and antisense probes were synthesized in vitro using T7 and SP6 RNA polymerase (Ambion). For fluorescence detection, probes were detected using peroxidase-labeled anti-DIG antibody, followed by tyramide signal amplification (Perkin Elmer) and incubation in 1:1000 AlexaFluor 594 streptavidin (Molecular Probes).

Immunofluorescence

Cultures were fixed in 4% formaldehyde, permeabilized in 0.1% Triton X-100 and blocked with 3% BSA. Incubation with primary antibody was carried out at 4°C overnight. Antibodies were used at the following concentrations: anti-PAM (Guo et al., 1998), 1:500; anti-PAM (Ehnert et al., 2004), 1:100; anti-Phospho-Tuberin (Ser939) (Cell Signaling Technology), 1:100; mouse anti-α-tubulin (Sigma), 1:2000. The cultures were washed several times in PBST and incubated with the appropriate secondary antibody (AlexaFluor 546 anti-rabbit, AlexaFluor 488 anti-rabbit or AlexaFluor 568 anti-mouse). They were then washed five times to remove unbound antibody.

Ligand binding assay

The membrane covering the lens of 4-day-old embryos was peeled off in PBS buffer. Fish embryos were incubated for 90 minutes in HBHA (Hanks buffered saline with 0.5 mg/ml BSA, 0.1% NaN_3, 20 mM HEPES, pH 7.0) containing 1 μg of zebrafish EphrinB2-human Fc chimera (R&D Systems). They were then washed five times with HBHA and fixed in acetone formaldehyde fixative. The embryos were washed four times with PBS pH 7.0 and blocked for 1 hour in PBST (containing 1% BSA and 0.1% Triton). Bound protein was detected using Alexa Fluor 488 anti-human IgG.

Lipofection

A dual-cassette plasmid containing a Gal4-VP16 transcriptional activator under the goldfish α-tubulin promoter and a tandem array of 14 UAS elements with a fish basal promoter driving expression of an *Unc76-EGFP* fusion was provided by the Fraser laboratory. The *Tα1:Gal4* cassette was excised and subcloned into pBluescript SKII, and the UAS cassette and plasmid backbone were recircularized. The α-tubulin promoter was replaced with the *HuC* promoter (Park et al., 2000). Lipofection procedures were based on that of *Xenopus* (Holt et al., 1990). Larvae were mounted in agarose at 30-hours post-fertilization and retinal cells were transfected by microinjection into the neural retina of the two plasmids (300-400 ng/μl) in 20% Neuroporter (Gene Therapy Systems).

Fluorescence imaging and quantitation

For fluorescently labeled embryos, samples were imaged with a Zeiss 510 LSM confocal microscope, using water immersion objectives. Tectal arbors were imaged with a 63× immersion objective. Measurements were made on projections using NIH ImageJ. Arborization area is the area of the convex polygon connecting axon tips to the first branch point. Maturity index is according to Schmidt et al. (Schmidt et al., 2004) and is defined as the total number of axon tips divided by highest order branch in that arbor (typically under 2.00 for immature arbors, up to 4.00 for very bushy arbors). Arborization area is underestimated owing to curvature of the tectum.

RGC cultures after antibody staining were imaged with a 20× phase objective on a Zeiss LSM510 confocal. Analysis was done using MetaMorph (Universal Imaging), Microsoft Excel and JMP IN (SAS Institute). Each channel was thresholded independently, and the distal-most 20 μm of each clearly individuated axon was traced, including any side branches or filopodia in this region. Axons were selected for analysis in the bright-field image without knowledge of genotype. Intensity of α-tubulin was used as a control for the measurement technique, and showed a roughly normal distribution and no differences between mutant and wild type. Statistical outliers (1.5×IQR method) for α-tubulin threshold area or intensity were excluded from analysis (seven out of 293 measurements). For combining data, intensity measurements were normalized to the wild type mean in each experiment. Results were the same for each individual experiment as for pooled data. Phospho-Tuberin measurements were not normally distributed, and were significantly different by Wilcoxon rank sum test ($P<0.0001$).

Results

Characterization of the *esrom* phenotype

The most prominent defect in the *esrom* mutant is a failure of anterior axons to map to the posterior tectum. In wild types, retinal axons from the anterior eye remain unbranched and are fasciculated until reaching the posterior tectum (Fig. 1A). In mutants, however, anterior axons branch in the anterior tectum (Fig. 1B). The posterior tectum is very sparsely innervated. Defects are also detectable in the dorsoventral axis of mutants. Axons from the ventral eye normally branch in the dorsal tectum, whereas those from the dorsal eye branch in the ventral tectum (Fig. 1C). In *esrom* mutants, this segregation is not strictly followed (Fig. 1D). In addition to these mapping errors, the pre-tectal target AF7 (Burrill and Easter, 1994) is excessively innervated in mutants, whereas fewer axons terminate in AF9 (Fig. 1E,F). Furthermore, axons are not bundled correctly in the optic nerve: axons that originate from one region of the eye and should therefore remain close together, are separated in mutants (Fig. 1G,H; split seen in all mutants, $n>50$, and in no wild types, $n>50$). The *esrom* gene is thus required for bundling, target selection and topographic mapping.

Whole eye transplantation (Fricke et al., 2001) was carried out between *esrom* mutants and wild types, and vice versa, to define where the *esrom* gene acts. Anterior axons from wild-type eyes branched only in the posterior tectum in *esrom* mutants (Fig. 2A). By contrast, axons from the anterior eye of *esrom* mutants branched anteriorly in the tectum of wild-type fish; additionally, strong innervation of AF7 was seen (Fig. 2B). Hence, *esrom* is required in the eye, and not in the brain, for normal branching and target selection of retinal axons. The effect of the *esrom* mutation was next examined in retinal cells in culture. No obvious difference was seen at initial stages of axon outgrowth (3-5 hours after explantation), with neurons extending individual axons in both wild-type and mutant cultures. After 24 hours, however, most wild-type retinal axons appeared to grow along one another in bundles, whereas many mutant axons still extended as individuals (Fig. 2C,D; see also Fig. 7). Preliminary time-lapse analysis indicates that these fascicles formed when retinal axons contacted one another and continued growing (see Movie 1 in the supplementary material). The ratio of fascicles to single axons in 24-hour-old cultures was found to be 1.97±0.55 for wild types and 0.46±0.15 for mutants. *esrom* thus appears to affect the formation of bundles in vitro. As in targeting and mapping, bundling appears to require the action of *esrom* in the eye, possibly in retinal axons themselves.

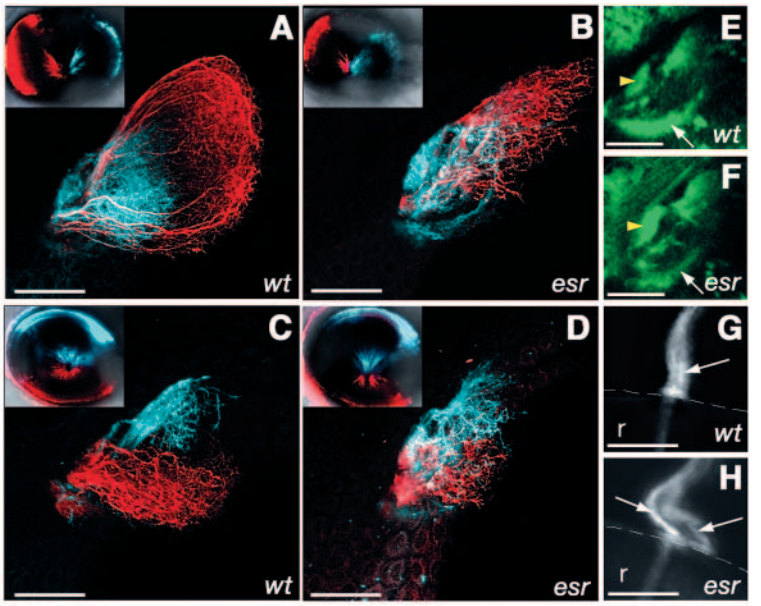

Fig. 1. The retinotectal projection in the *esrom* mutant. (A-D) Optic tectum of 4-day-old zebrafish, with retinal axons labeled using DiI (red) or DiD (blue). Insets show lateral view of the injected eye. (A) Axons from the anterior region of the eye (red) project to the posterior tectum in wild type. Axons from the posterior (blue) arborize in the anterior tectum. (B) In the *esrom* mutant, anterior axons defasciculate and arborize anteriorly. (C) Axons from the ventral (red) and dorsal (blue) regions of the eye are well separated in a wild type. (D) In the mutant, there is some overlap between two populations. (E,F) Dorsal view of the pretectal region of 3-day-old fish, in which retinal axons are labeled with GFP under the sonic hedgehog promoter. The pretectal target AF7 (yellow arrowhead) is more innervated in the mutant (F) compared with the wild type (G). AF9 (arrow), by contrast, is less innervated in the mutant. (G,H) The optic nerve exiting from the eye in 7-day-old fish. Only dorsal neurons have been labeled with DiI. In the wild type (G), axons remain closely associated with one another in the optic nerve (arrow). In the mutant (H), axons have formed two separate bundles (arrows). Scale bar: 50 μm. Anterior is towards the left. r, retina; the broken white line in G,H indicates the margin of the eye. (E,F) Single optical planes; other panels are projections of *z*-stacks.

Positional cloning of *esrom*

We identified the *esrom* gene by positional cloning. Initial linkage to the centromeric region of chromosome 9 was determined by bulked segregation analysis. *esrom* is flanked by two microsatellite markers Z6663 (0.5 cM) and z7813 (2.3 cM) (Fig. 3A). The 5′ and 3′ untranslated ends of expressed sequenced tags (ESTs) were used preferentially to generate SSCP (simple sequence conformation polymorphism) markers for fine mapping. The gene mapped 0.2 cM from fj33d03 and less than 0.08 cM from fa97c06. These ESTs were then used to screen zebrafish genomic PAC and BAC libraries to build a contig encompassing the gene (Fig. 3B). The entire contig was shotgun sequenced. The contig assembly revealed that the *esrom* locus was highly syntenic to human chromosome 13q22.3, which harbors *CLN5*, *BTF3L1*, *FBXL3a*, a large gene *PAM* (protein associated with Myc) and sciellin. Orthologs of *PAM* (Guo et al., 1998) in *Drosophila* and *C. elegans* play an important role in axonal branching and synapse maturation (Schaefer et al., 2000; Wan et al., 2000; Zhen et al., 2000). The zebrafish *PAM* ortholog was knocked down using antisense morpholinos targeted to two predicted splice sites (Draper et al., 2001). Embryos injected with either of these morpholinos mimicked both the retinotectal and pigment phenotypes (Odenthal et al., 1996) of *esrom* mutants (Fig. 3C-H), suggesting that *esrom* is the zebrafish ortholog of *PAM/highwire/rpm-1*.

Three subclones of the putative *esrom* gene were represented in the zebrafish EST project database: fc79d04 (26-somite embryos, adult liver, shield stage embryos), fa97c06 (fin day 3 regeneration library) and fv19f02 (adult brain library). The 5′ end of the gene was cloned using 5′ RACE, to clarify inconsistencies in the contig assembly. The full-length transcript is 14224 bp (Accession Number, AY818192), as deduced from two overlapping subclones (13kb and 1.28 kb) obtained from 2-4 day embryonic cDNA. Splice variants were not seen during early embryonic development (Fig. 3I). The gene size is estimated to be at least 250 kb. To molecularly characterize the lesion in *esrom* alleles, we sequenced cDNA. esr^{tpO3} has a single nucleotide change from T to A that changes cysteine at position 4289 to serine (Fig. 3J). The esr^{te50} transcript has a 110-nucleotide deletion in the basic rich region within the RCC1 domain and esr^{te75} has a 24-nucleotide insertion, which is proline rich, in the same domain. The presence of these alterations in the cDNA of three *esrom* alleles, together with the mapping and morpholino data, establishes the identity of *esrom*.

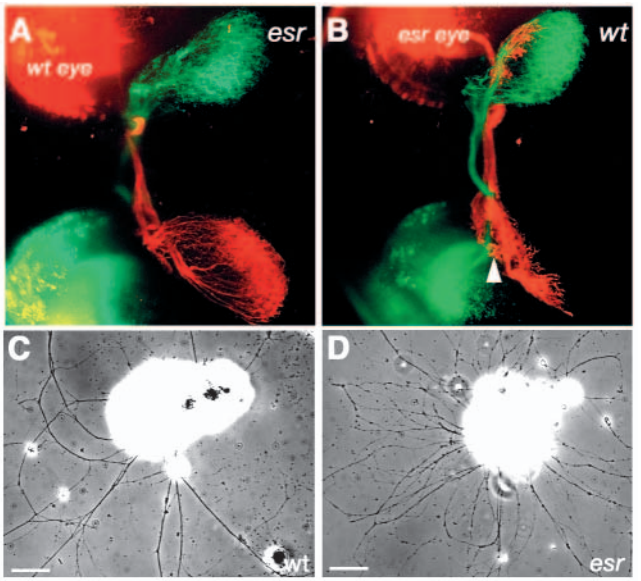

Fig. 2. Autonomy of *esrom* gene function. (A) Transplantation of a wild-type eye into a mutant host. Axons from the anterior region of the wild-type eye (red) remain fasciculated and project to the posterior tectum. Axons from the host eye (green) branch aberrantly and are not tightly fasciculated in the optic tract. (B) Transplantation of a mutant eye into a wild-type host. Axons from the anterior region of the host eye (green) project to the posterior tectum, whereas those from the mutant eye (red) terminate in the anterior tectum. AF7 is indicated by the arrowhead. (C) Wild-type retinal axons fasciculate in vitro. (D) Mutant axons do not fasciculate as strongly. Scale bar: 50 μm. Anterior is towards the left.

The Esrom protein

Esrom is a multidomain protein (Fig. 4A) with potential leucine zippers LZ1and LZ2, an unusual RCC1 (regulator of chromatin condensation)-like domain (674-1052) interrupted by a basic rich region (BR), PHR repeat regions, filamin repeats (2335-2428), a region similar to the Myc-binding region of PAM (truncated by 75 amino acids), a histone-binding region (HHD), a serine-rich region (SR), a nuclear localization sequence (3093-3112), a B-box zinc finger (4154-4199), a C3HC4 type RING zinc finger (4324-4375), a cytochrome heme binding region (4513-4518), a LDLRA1 (low-density lipoprotein receptor class A) motif (4302-4327) and a bHLH (basic helix-loop-helix) Myc type dimerization domain (4021- 4036).

One highly conserved region in Esrom is the C terminus, which contains the B-box and RING finger. The presence of a RING finger, which can associate with an E2 ubiquitin-conjugating enzyme (Lorick et al., 1999), and the fact that *highwire* genetically interacts with *fat facets* (DiAntonio et al., 2001), which encodes a deubiquitinating enzyme, suggests that Esrom can function as an E3 ligase. Indeed, the purified C terminus of Esrom, consisting of the RING finger and downstream sequences, has auto-ubiquitinating activity in the presence of Ubiquitin, E1 and the E2 UbcH5b (Fig. 4C). The *esr*^{tp03} allele, which has a mutation in a residue that is conserved from *C. elegans* to humans and is important in the formation of a disulphide bridge, suggests that the C terminus is important for retinal axon targeting. In support of this, the morpholino that targets a splice donor site upstream of the B-box also led to a retinotectal phenotype (Fig. 3C,D). Another domain of Esrom, the PHR repeat, is also highly conserved. This domain is found in a subset of BTB/POZ family proteins, which can act as substrate specificity adaptors for Cul3-based ubiquitin ligases (Furukawa et al., 2003; Xu et al., 2003a). Additionally, the PHR-containing proteins BTBD1 and BTBD2 colocalize with TRIM5δ, a RING protein with domain architecture similar to the Esrom C terminus (Xu et al., 2003b). Hence, one potential function of Esrom in the retinotectal projection is as an E3 ligase.

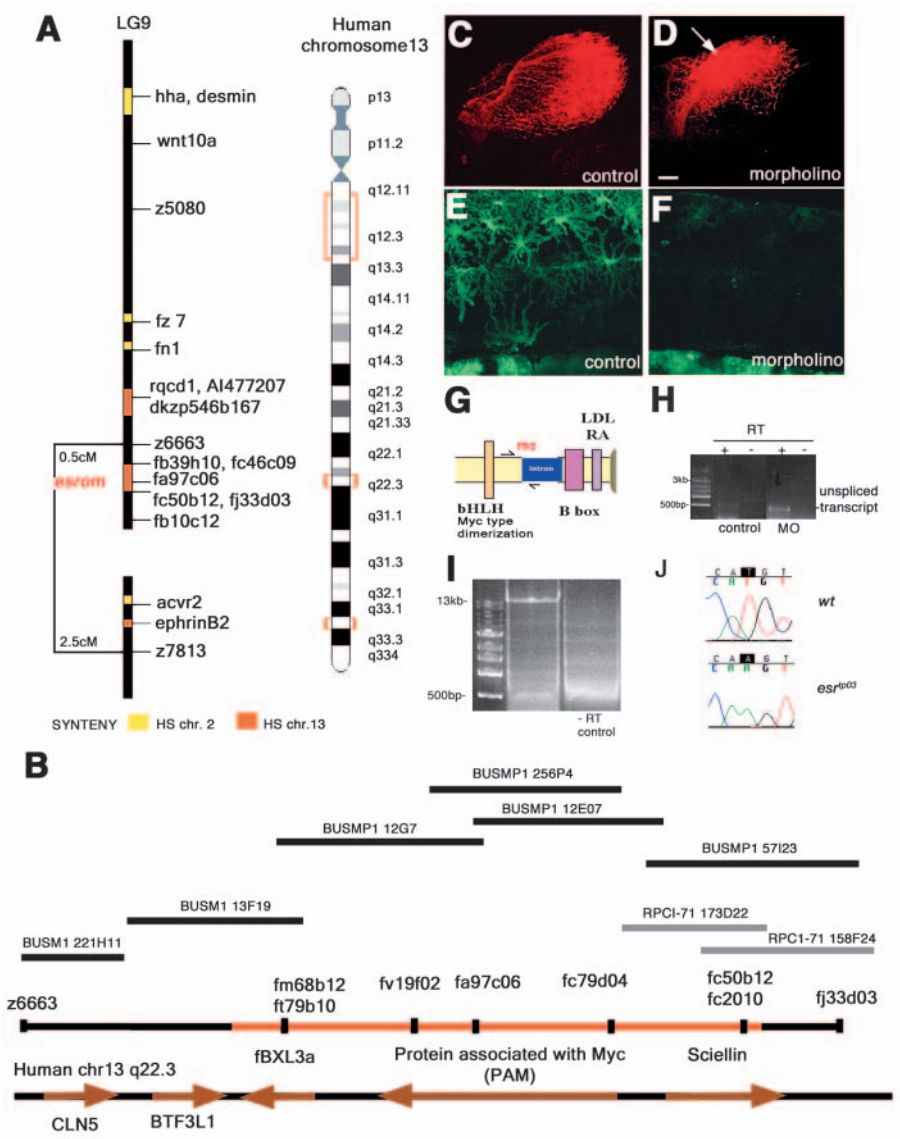

Fig. 3. Positional cloning of *esrom*. (A) Map of zebrafish chromosome 9, depicting the region to which *esrom* maps and its synteny to human chromosome 13 (orange). Yellow color indicates synteny to human chromosome 2. (B) Genomic contig assembly of zebrafish PAC and BAC clones encompassing *esrom* and its similarity to human chromosome 13q22.3. *esr* maps 0.5 cM from z6663, 0.2 cM from fj33d03 and less than 0.08 cM from fa97c06. (C,D) Retinotectal projections of DiI-labeled anterior RGC axons in 4-day-old wild-type embryos injected with control morpholino and zebrafish PAM morpholino. (C) In the control, anterior RGC axons branch in the posterior tectum as in wild types. (D) In zebrafish, PAM morphants anterior RGC axons branch prematurely in the anterior tectum (arrow). (E,F) Lateral view of 3-day-old larvae. Xanthophore phenotype in morphants mimics that of mutants (Le Guyader et al., 2004). (G) Splice site target of zebrafish PAM morpholino2. (H) RT-PCR of 400 bp unspliced transcript in control and morphants. The unspliced band is amplified only in the zebrafish PAM morphants. (I) Single cDNA band (13 kb) from RT-PCR using *esrom* specific primers. (J) Point mutation in *esr*^{tp03}. Scale bar: 25 μm.

Localization of Esrom

The *esrom* gene is widely expressed when the visual system begins developing, as determined by in situ hybridization (Fig. 4D,E). In the eye, *esrom* appears to be transcribed in all cells, including retinal ganglion cells, with no obvious gradient (Fig. 4F,G). To determine the distribution of the Esrom protein, an antibody made to the highly conserved C terminus of PAM (Guo et al., 1998) was used. This antibody, which binds to the C terminus of Esrom (Fig. 4H), recognizes a single high molecular weight zebrafish protein (Fig. 4I). When used for immunofluorescence,

punctate label was detected in retinal ganglion cells, including in lamellipodia and filopodia (Fig. 4J-M). A second antibody to PAM (Ehnert et al., 2004) also gave similar punctate labeling. When this antibody was pre-absorbed with a peptide from the corresponding region of the zebrafish Esrom protein, a reduction in fluorescence intensity was seen (Fig. 4N,O). Taken together, these data indicate that Esrom protein is present in retinal axons. The puncta are similar to cytoplasmic bodies formed by other B-box and RING finger-containing proteins and is likely to reflect supramolecular assemblies formed by these domains (Borden et al., 1996; Kentsis et al., 2002). The localization of the Esrom protein suggests that it functions in retinal ganglion cells, possibly in growth cones.

Branching in retinal axons

The *Drosophila highwire* mutant has increased branching of

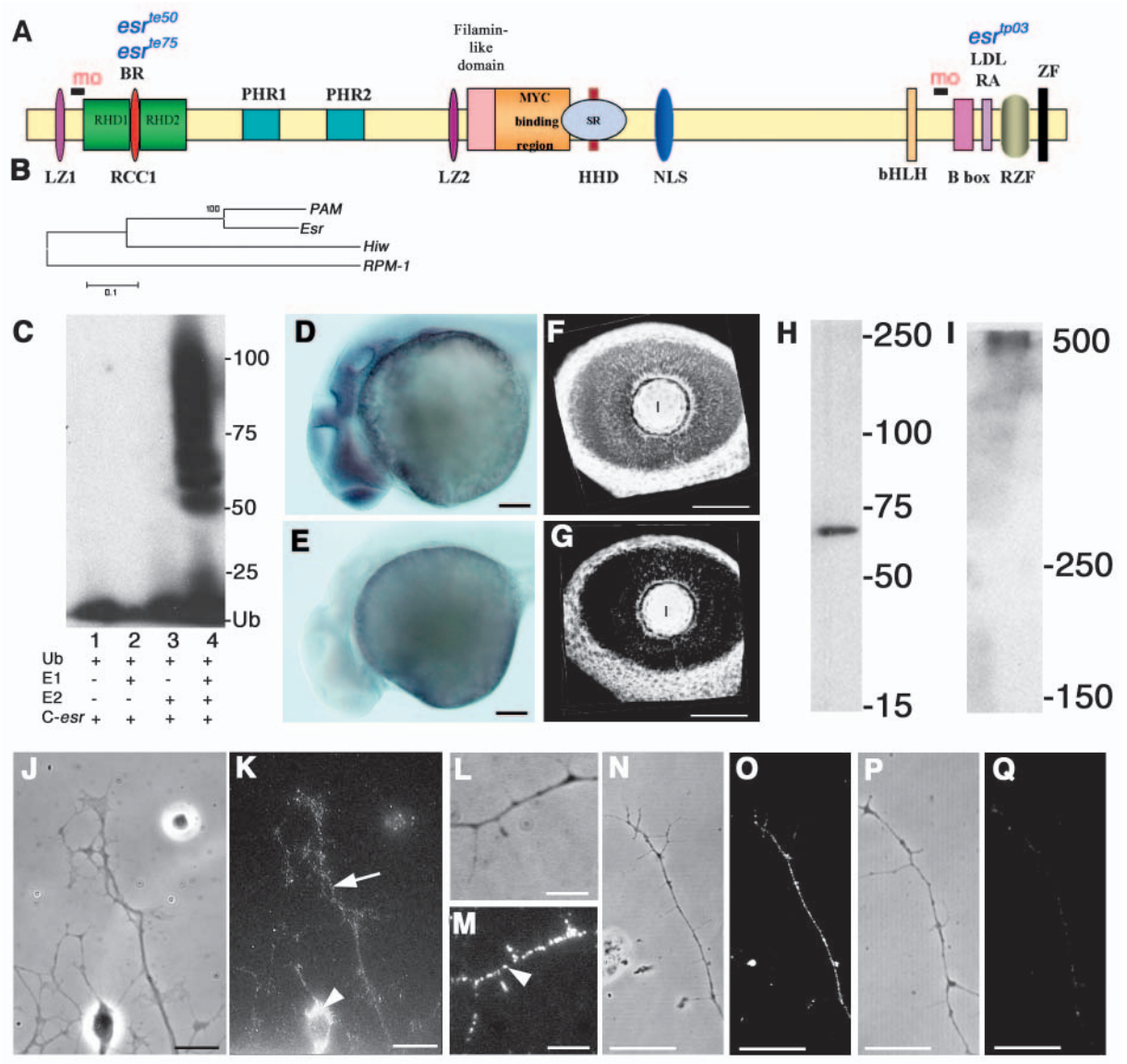

Fig. 4. The *esrom* gene. (A) Predicted domains in Esrom. See text for full description. *mo* represents target sites for morpholinos. The positions of three mutations are indicated above the protein. (B) Esrom is phylogenetically closer to human PAM than *Drosophila* HIW and *C. elegans* RPM-1. (C) E3 ligase activity of 45 kDa Esrom C terminus containing the RING finger. Lanes 1-3 are controls. Lane 4 shows protein polyubiquitination in the presence of E1, E2 (UbcH5b) and Ub. (D,E) In situ hybridization with 30-hour-old zebrafish, shown here in lateral view. The antisense probe to *esrom* shows widespread label, with signal visible in all regions of the brain (D); no signal was detected with a sense probe (E). (F,G) Three-dimensional reconstructions of the eye of 48-hour-old fish labeled with antisense (F) or sense (G) probes to *esrom*, showing a lateral view. The gene is expressed uniformly in the developing retina. Lens labeling is nonspecific. (H,I) Western blot using a C terminus specific anti-PAM antibody. The antibody recognizes the 67 kDa C terminus end of Esrom (H), which is 98% identical to PAM, and a single 500 kDa protein from zebrafish embryo extract (I). (J-M) Esrom localization in retinal cells in vitro. (J,K) Label is detectable in the cytoplasm (arrowhead) and entire axon (arrow). Puncta are visible at high magnification (M, arrowhead). (J,L) Phase images; (K,M) the corresponding fluorescence images. (N-Q) Pre-absorption control; both axons were imaged at identical settings on a confocal microscope. (N,O) Without pre-absorption, the entire axon was labeled. (P,Q) With pre-absorption, very weak label was detected. Scale bar: 5 μm in L,M; 10 μm in J,K,N-Q; 100 μm in D-G; l, lens.

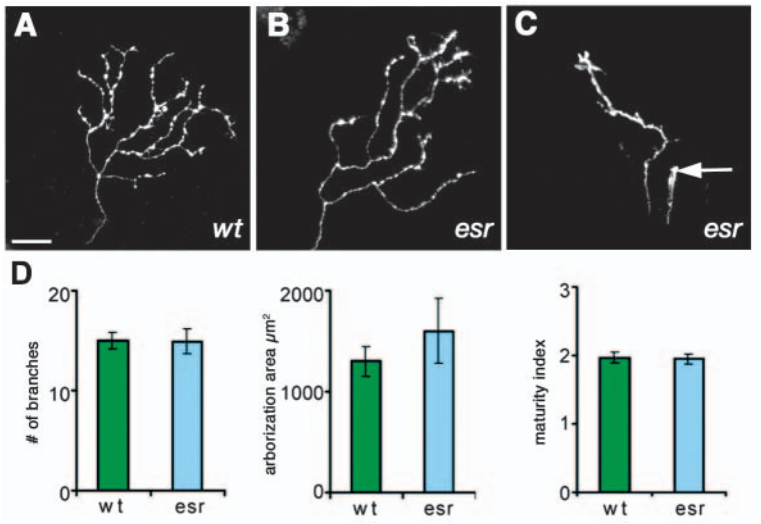

Fig. 5. Branching in the retinal axons. Tectal arbors of RGCs expressing *unc76-egfp* in 4-day-old wild type (A) and mutant (B) are similar, with no measurable differences in branch number, arborization area or maturity index (D, error bars=s.e.m.). A subset of mutant axons stop near the tectal entry point at 3 days and do not arborize (C, arrow); the axon on the left was seen to arborize normally subsequently. Scale bar: 10 μm.

motoneurons at the neuromuscular junction (Wan et al., 2000). Surprisingly, *esrom* mutant retinal axons did not show increased branching. This could be seen when individual retinal ganglion cells were labeled by lipofection with an *unc76-eGFP* fusion construct (Fig. 5A-C) and their arbors measured. No difference could be detected between the tectal arborizations of mutant and wild-type axons in terms of number of branches, area or maturity index, a measure of arbor bushiness (Schmidt et al., 2004), at 4 days post-fertilization (Fig. 5D). Although the lipofection of RGCs was equally efficient in mutants and wild type, tectal arbors often never appeared in *esrom*. Whole-mount staining with the Zn8 antibody confirmed that fewer axons reach the tectum (data not shown). Esrom is thus required to ensure that retinal axons reach the tectum and that they branch in the appropriate position; it does not regulate the amount of branching during map formation.

Positional identity in the retina

Esrom could influence the retinotectal projection at multiple levels. There may be a patterning defect in the eye: in light of its potential interaction with Myc, Esrom could regulate transcriptional events that pattern the retina. However, differentiation of the retina, which occurs in a wave from the ventronasal quadrant, appears similar in *esrom* mutants and wild types, as analyzed using a *sonic hedgehog:eGFP* reporter (data not shown). Additionally, EphrinB2-fc, a useful marker of polarity, as it labels the eye in a graded fashion with a maximum at the posteroventral region, binds to mutant and wild-type retina in a similar manner (Fig. 6). These observations, and the fact that the overall map formed on the mutant tectum is roughly correct, albeit compressed, suggest that there is no gross patterning defect in the retina.

Signal transduction in retinal axons

An alternative possibility is that Esrom is required to regulate intracellular signaling pathways that regulate axon growth and guidance. The conserved C terminus of the human Esrom ortholog PAM physically interacts with the tumor suppressor Tuberin, and PAM and Tuberin colocalize in puncta in mammalian axons and growth cones (Murthy et al., 2004). Tuberin is encoded by the *TSC2* gene and, with its dimerization partner Hamartin (*TSC1*), is an important regulator of the Target of Rapamycin (TOR) protein synthesis pathway (Li et al., 2004). In addition, they can affect processes such as cell adhesion, motility, actin cytoskeleton (Lamb et al., 2000; Astrinidis et al., 2002) and plasma membrane composition (Kleymenova et al., 2001; Jones et al., 2004). Tuberin is under complex regulation, and contains multiple known and predicted target sites for various kinases. Phosphorylation of Tuberin generally leads to impairment of its function through dissociation from Hamartin, sequestration by 14-3-3 proteins, ubiquitination or some combination of these events (Krymskaya, 2003).

The region of Tuberin required for PAM interaction contains a conserved serine (Ser939), which is phosphorylated by at least two distinct pathways. Akt/PKB phosphorylates Ser939 as a result of activation of the PI(3)-kinase pathway, as does RSK1 in response to protein kinase C (PKC) and MEK-dependent signaling, though to a lesser extent than Akt (Dan et al., 2002; Inoki et al., 2002; Manning et al., 2002; Potter et al., 2002; Tee et al., 2003a; Roux et al., 2004). An antibody specific to Ser939 Phospho-Tuberin revealed a heterogeneous distribution in both wild-type and mutant retinal axons (Fig. 7A). Many axons contained an enrichment of Phospho-Tuberin in the most distal 10-20 μm, including active and collapsed growth cones. In axon shafts, Phospho-Tuberin often localized to large varicosities, branch points and at sites of inter-axonal contact.

Because it appeared that mutant retinal explants showed intense focal enrichments of Phospho-Tuberin antibody staining at axon tips (Fig. 7), we focused on the distal-most 20 μm of RGC axons and measured fluorescence intensity. As this region varies from axon to axon in several morphological criteria, the intensity of α-tubulin antibody staining was used as a measurement control (see Materials and methods for quantitation details). Phospho-Tuberin levels were found to be significantly higher in mutant axons (Fig. 7C), while α-tubulin levels were similar.

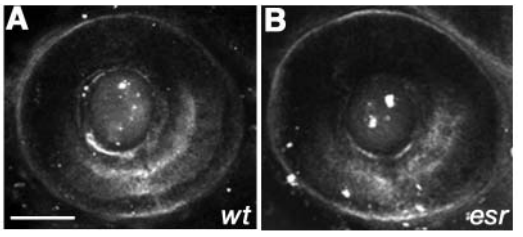

Fig. 6. In situ binding of EphrinB2-fc in the eye of a 4-day-old wild type (A) and *esr*^{te50} (B) embryo. Scale bar: 20 μm; eye is shown in lateral view, with anterior towards the left.

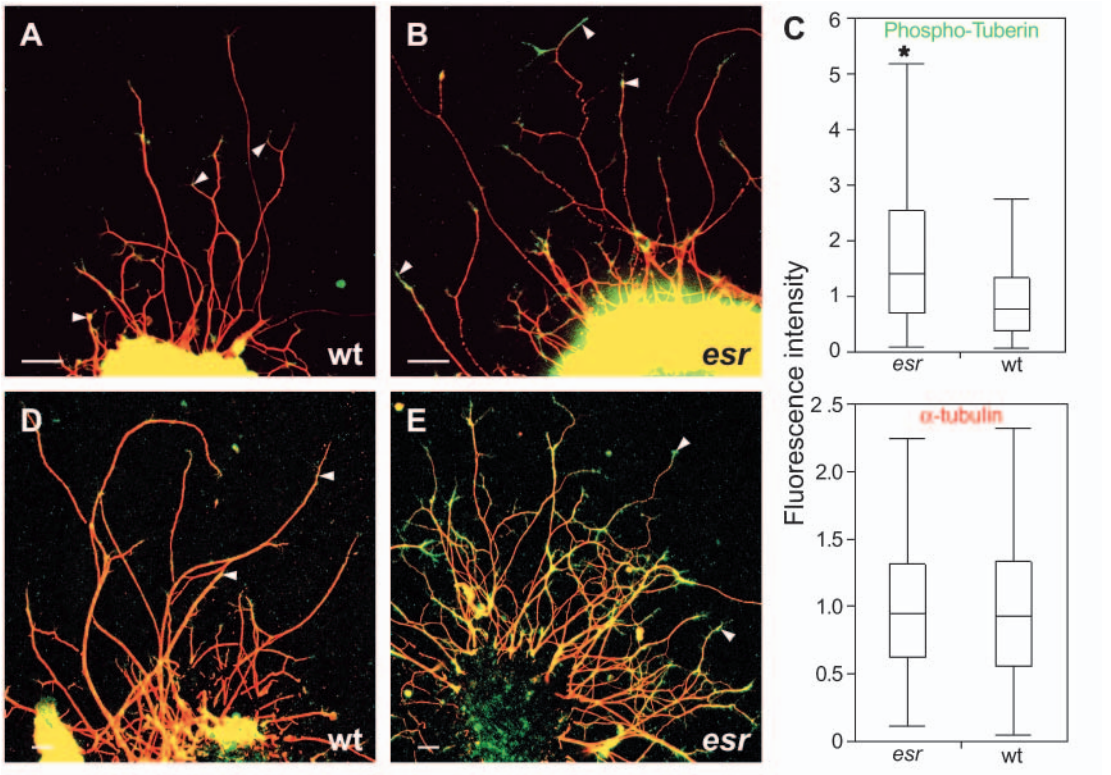

Fig. 7. Ser939 Phospho-Tuberin (green) and α-tubulin (red) immunofluorescence in retinal explants. (A) After 15 hours in culture, Phospho-Tuberin (arrowheads) is detected in retinal axons, with higher levels in the *esrom* mutant (B). (C) At this time, Phospho-Tuberin immunofluorescence is twofold higher on average in *esrom* axon tips (*P<0.0001); box plot shows medians and quartiles from two normalized independent experiments (n_{wt}=83, n_{esr}=99 and n_{wt}=26, n_{esr}=78). After 26 hours in culture, the fasciculation phenotype is apparent, and Phospho-Tuberin staining difference is intensified. Scale bar: 50 μm.

Discussion

By positional cloning, allele sequencing and morpholino injection, we have established that Esrom is an ortholog of PAM/Highwire/RPM-1. PAM was initially identified in a biochemical screen for proteins interacting with Myc (Guo et al., 1998), while RPM-1 and Highwire were identified in screens for genes involved in neural development (Schaefer et al., 2000; Wan et al., 2000; Zhen et al., 2000). In contrast to *highwire*, the function of *esrom* is not restricted to regulation of branching and synaptogenesis of neurons. Instead, *esrom* is also required in the visual system for correct fasciculation, targeting and mapping of retinal axons. *esrom*, like the mouse ortholog *Phr1* (Burgess et al., 2004), is widely expressed, being found in both neural and non-neural cells (J. D'Souza, unpublished), whereas *highwire* (Wan et al., 2000) and *rpm-1* (Schaefer et al., 2000) are essentially neural specific. Unlike *rpm-1* and *highwire*, *esrom* mutations are lethal. These differences, which may reflect a general difference between vertebrate and inverebrate orthologs, suggest that this gene has acquired additional capabilities during evolution, enabling it to perform different functions in different situations. A clear example of this is in the xanthophores, where *esrom* is required to regulate pteridine synthesis (Le Guyader et al., 2004).

We observed that the tumor suppressor and intracellular signaling molecule Tuberin is misregulated in *esrom* mutant axons. Although Tuberin and its binding partner Hamartin are known to localize to axons and growth cones, it is not clear what role they play in axon growth and guidance. The elevated levels of Ser939-phosphorylated Tuberin could be explained in several ways. Although we currently lack the data to distinguish conclusively between these possibilities, each scenario predicts different effects on processes known to be downstream of Tuberin. In one scenario, Esrom could modulate signaling pathways upstream of Tuberin, in which case the hyperphosphorylation in mutants should lead to a decrease in Tuberin function and an increase in activitation of the TOR pathway. Alternatively, there may simply be more Tuberin in mutants, and thus a proportional increase in Phospho-Tuberin; this predicts an overabundance of functional Tuberin and a downregulation of the TOR pathway. Yet another possibility is that phosphorylated Tuberin is normally turned over rapidly, via dephosphorylation or degradation, for example; this process is disrupted in mutants. Because phosphorylated Tuberin can be functionally inhibited by mechanisms other than degradation, it is not clear what effects the accumulation of Phospho-Tuberin might have in this case.

It remains to be determined if the misregulation of Tuberin contributes to the retinotectal phenotype observed in *esrom* mutants. The best-characterized role of Tuberin is as a regulator of protein synthesis (Inoki et al., 2003; Tee et al., 2003b). The localized translation of mRNAs is required for growth cone responses to certain guidance cues, as well as for adaptive resensitization during chemotaxis (Campbell and Holt, 2001; Ming et al., 2002). Transcripts that have been found in axons of diverse neuronal types include β-actin and other cytoskeletal components (Piper and Holt, 2004), which are key regulatory targets for axon guidance cues. EphA2, a receptor tyrosine kinase involved in topographic mapping, has been shown to be under translational regulation in axons as well (Brittis et al., 2002). However, in addition to protein synthesis, Tuberin and Hamartin regulate other cellular processes that could potentially affect axon guidance and fasciculation.

Orthologs of Esrom have been recently implicated in seemingly diverse processes. In *C. elegans,* RPM-1 forms an

SCF-type E3 ligase complex that may regulate an insulin superfamily receptor, anaplastic lymphoma kinase (Liao et al., 2004). In *Drosophila*, Highwire binds the fly co-SMAD Medea and influences BMP signaling (McCabe et al., 2004). Finally, in mammalian cells, the membrane localization of PAM has been shown to be regulated by signaling downstream of G-protein coupled receptors that recognize the phospholipid sphingosine 1-phosphate (Pierre et al., 2004). This is essential for the potent and long-term inhibition of adenylate cyclase by PAM. The ability of PAM to regulate adenylate cyclase (Scholich et al., 2001), which is presumably shared by Esrom (as the RCC1 homology domain is conserved), is particularly interesting, as cAMP levels are important modulators of growth cone responses to guidance cues (Ming et al., 1997; Song et al., 1997).

In conclusion, by positional cloning and analysis of the zebrafish *esrom* mutant, we have identified a large protein with multiple domains, which is needed for the accurate response of retinal growth cone to cues in vivo. Growth cone navigation requires a complex network of interacting signal transduction pathways that affect diverse subcellular processes in highly dynamic and localized ways. It is interesting to speculate that the large size and multiple interactions of Esrom and its orthologs allow it to serve as a network hub that coordinates a set of signaling processes important in various neuronal contexts, including axon guidance, synaptic growth and neurophysiology. Esrom can perhaps be viewed as a microprocessor, enabling the simultaneous control of different processes in response to multiple inputs. In the case of the retinotectal projection, Esrom could be a component of a coincidence detector that matches position on the tectum to identity of the cell, helping the axon to grow and to branch where appropriate.

We thank Alan Coulson and the Sanger Center for sequencing the *esrom* contig; Qingbin Guo for the PAM antibody; Reinhardt Koster and Scott Fraser for the Gal4-UAS construct; Connie Er for imaging assistance; and Friedrich Bonhoeffer for providing the opportunity to start this work. The National Science and Technology Board of Singapore and the Temasek Life Sciences Laboratory funded this project. Initial stages were supported by the Human Frontiers Science Program and Max Planck Society fellowships to S.J.

Supplementary material

Supplementary material for this article is available at
http://dev.biologists.org/cgi/content/full/132/2/247/DC1

References

Astrinidis, A., Cash, T. P., Hunter, D. S., Walker, C. L., Chernoff, J. and Henske, E. P. (2002). Tuberin, the tuberous sclerosis complex 2 tumor suppressor gene product, regulates Rho activation, cell adhesion and migration. *Oncogene* **21**, 8470-8476.

Baier, H., Klostermann, S., Trowe, T., Karlstrom, R. O., Nusslein-Volhard, C. and Bonhoeffer, F. (1996). Genetic dissection of the retinotectal projection. *Development* **123**, 415-425.

Borden, K. L., Lally, J. M., Martin, S. R., O'Reilly, N. J., Solomon, E. and Freemont, P. S. (1996). In vivo and in vitro characterization of the B1 and B2 zinc-binding domains from the acute promyelocytic leukemia protooncoprotein PML. *Proc. Natl. Acad. Sci. USA* **93**, 1601-1606.

Brittis, P. A., Lu, Q. and Flanagan, J. G. (2002). Axonal protein synthesis provides a mechanism for localized regulation at an intermediate target. *Cell* **110**, 223-235.

Burgess, R. W., Peterson, K. A., Johnson, M. J., Roix, J. J., Welsh, I. C. and O'Brien, T. P. (2004). Evidence for a conserved function in synapse formation reveals Phr1 as a candidate gene for respiratory failure in newborn mice. *Mol. Cell. Biol.* **24**, 1096-1105.

Burrill, J. D. and Easter, S. S., Jr (1994). Development of the retinofugal projections in the embryonic and larval zebrafish (Brachydanio rerio). *J. Comp. Neurol.* **346**, 583-600.

Campbell, D. S. and Holt, C. E. (2001). Chemotropic responses of retinal growth cones mediated by rapid local protein synthesis and degradation. *Neuron* **32**, 1013-1026.

Dan, H. C., Sun, M., Yang, L., Feldman, R. I., Sui, X. M., Ou, C. C., Nellist, M., Yeung, R. S., Halley, D. J., Nicosia, S. V. et al. (2002). Phosphatidylinositol 3-kinase/Akt pathway regulates tuberous sclerosis tumor suppressor complex by phosphorylation of tuberin. *J. Biol. Chem.* **277**, 35364-35370.

DiAntonio, A., Haghighi, A. P., Portman, S. L., Lee, J. D., Amaranto, A. M. and Goodman, C. S. (2001). Ubiquitination-dependent mechanisms regulate synaptic growth and function. *Nature* **412**, 449-452.

Draper, B. W., Morcos, P. A. and Kimmel, C. B. (2001). Inhibition of zebrafish fgf8 pre-mRNA splicing with morpholino oligos: a quantifiable method for gene knockdown. *Genesis* **30**, 154-156.

Ehnert, C., Tegeder, I., Pierre, S., Birod, K., Nguyen, H. V., Schmidtko, A., Geisslinger, G. and Scholich, K. (2004). Protein associated with Myc (PAM) is involved in spinal nociceptive processing. *J. Neurochem.* **88**, 948-957.

Foemzler, D. and Beier, D. (1999). Gene Mapping in Zebrafish Using Single-Strand Conformation Polymorphism Analysis. In *The zebrafish: genetics and genomics*, Vol. 60 (ed. H. Detrich, M. Westerfield and L. Zon), San Diego, CA: Academic Press.

Fricke, C., Lee, J. S., Geiger-Rudolph, S., Bonhoeffer, F. and Chien, C. B. (2001). astray, a zebrafish roundabout homolog required for retinal axon guidance. *Science* **292**, 507-510.

Furukawa, M., He, Y. J., Borchers, C. and Xiong, Y. (2003). Targeting of protein ubiquitination by BTB-Cullin 3-Roc1 ubiquitin ligases. *Nat. Cell Biol.* **5**, 1001-1007.

Guo, Q., Xie, J., Dang, C. V., Liu, E. T. and Bishop, J. M. (1998). Identification of a large Myc-binding protein that contains RCC1-like repeats. *Proc. Natl. Acad. Sci. USA* **95**, 9172-9177.

Hindges, R., McLaughlin, T., Genoud, N., Henkemeyer, M. and O'Leary, D. D. (2002). EphB forward signaling controls directional branch extension and arborization required for dorsal-ventral retinotopic mapping. *Neuron* **35**, 475-487.

Holt, C. E., Garlick, N. and Cornel, E. (1990). Lipofection of cDNAs in the embryonic vertebrate central nervous system. *Neuron* **4**, 203-214.

Inoki, K., Li, Y., Zhu, T., Wu, J. and Guan, K. L. (2002). TSC2 is phosphorylated and inhibited by Akt and suppresses mTOR signalling. *Nat. Cell Biol.* **4**, 648-657.

Inoki, K., Li, Y., Xu, T. and Guan, K. L. (2003). Rheb GTPase is a direct target of TSC2 GAP activity and regulates mTOR signaling. *Genes Dev.* **17**, 1829-1834.

Jones, K. A., Jiang, X., Yamamoto, Y. and Yeung, R. S. (2004). Tuberin is a component of lipid rafts and mediates caveolin-1 localization: role of TSC2 in post-Golgi transport. *Exp. Cell Res.* **295**, 512-524.

Karlstrom, R. O., Trowe, T., Klostermann, S., Baier, H., Brand, M., Crawford, A. D., Grunewald, B., Haffter, P., Hoffmann, H., Meyer, S. U. et al. (1996). Zebrafish mutations affecting retinotectal axon pathfinding. *Development* **123**, 427-438.

Kentsis, A., Gordon, R. E. and Borden, K. L. (2002). Control of biochemical reactions through supramolecular RING domain self-assembly. *Proc. Natl. Acad. Sci. USA* **99**, 15404-15409.

Kleymenova, E., Ibraghimov-Beskrovnaya, O., Kugoh, H., Everitt, J., Xu, H., Kiguchi, K., Landes, G., Harris, P. and Walker, C. (2001). Tuberin-dependent membrane localization of polycystin-1: a functional link between polycystic kidney disease and the TSC2 tumor suppressor gene. *Mol. Cell* **7**, 823-832.

Krymskaya, V. P. (2003). Tumour suppressors hamartin and tuberin: intracellular signalling. *Cell. Signal.* **15**, 729-739.

Lamb, R. F., Roy, C., Diefenbach, T. J., Vinters, H. V., Johnson, M. W., Jay, D. G. and Hall, A. (2000). The TSC1 tumour suppressor hamartin regulates cell adhesion through ERM proteins and the GTPase Rho. *Nat. Cell Biol.* **2**, 281-287.

Le Guyader, S., Maier, J. and Jesuthasan, S. (2004). Esrom, an ortholog of PAM/Hiw/Rpm-1, regulates pteridine synthesis in the zebrafish. *Dev. Biol.* (in press).

Li, Y., Corradetti, M. N., Inoki, K. and Guan, K. L. (2004). TSC2: filling the GAP in the mTOR signaling pathway. *Trends Biochem. Sci.* **29**, 32-38.

Liao, E. H., Hung, W., Abrams, B. and Zhen, M. (2004). An SCF-like ubiquitin ligase complex that controls presynaptic differentiation. *Nature* **430**, 345-350.

Lorick, K. L., Jensen, J. P., Fang, S., Ong, A. M., Hatakeyama, S. and Weissman, A. M. (1999). RING fingers mediate ubiquitin-conjugating enzyme (E2)-dependent ubiquitination. *Proc. Natl. Acad. Sci. USA* **96**, 11364-11369.

Mann, F., Ray, S., Harris, W. and Holt, C. (2002). Topographic mapping in dorsoventral axis of the Xenopus retinotectal system depends on signaling through ephrin-B ligands. *Neuron* **35**, 461-473.

Manning, B. D., Tee, A. R., Logsdon, M. N., Blenis, J. and Cantley, L. C. (2002). Identification of the tuberous sclerosis complex-2 tumor suppressor gene product tuberin as a target of the phosphoinositide 3-kinase/akt pathway. *Mol. Cell* **10**, 151-162.

McCabe, B. D., Hom, S., Aberle, H., Fetter, R. D., Marques, G., Haerry, T. E., Wan, H., O'Connor, M. B., Goodman, C. S. and Haghighi, A. P. (2004). Highwire regulates presynaptic BMP signaling essential for synaptic growth. *Neuron* **41**, 891-905.

Ming, G. L., Song, H. J., Berninger, B., Holt, C. E., Tessier-Lavigne, M. and Poo, M. M. (1997). cAMP-dependent growth cone guidance by netrin-1. *Neuron* **19**, 1225-1235.

Ming, G. L., Wong, S. T., Henley, J., Yuan, X. B., Song, H. J., Spitzer, N. C. and Poo, M. M. (2002). Adaptation in the chemotactic guidance of nerve growth cones. *Nature* **417**, 411-418.

Murthy, V., Han, S., Beauchamp, R. L., Smith, N., Haddad, L. A., Ito, N. and Ramesh, V. (2004). Pam and its ortholog highwire interact with and may negatively regulate the TSC1.TSC2 complex. *J. Biol. Chem.* **279**, 1351-1358.

Neumann, C. J. and Nuesslein-Volhard, C. (2000). Patterning of the zebrafish retina by a wave of sonic hedgehog activity. *Science* **289**, 2137-2139.

Odenthal, J., Rossnagel, K., Haffter, P., Kelsh, R. N., Vogelsang, E., Brand, M., van Eeden, F. J., Furutani-Seiki, M., Granato, M., Hammerschmidt, M. et al. (1996). Mutations affecting xanthophore pigmentation in the zebrafish, Danio rerio. *Development* **123**, 391-398.

Orike, N. and Pini, A. (1996). Axon guidance: following the Eph plan. *Curr. Biol.* **6**, 108-110.

Park, H. C., Kim, C. H., Bae, Y. K., Yeo, S. Y., Kim, S. H., Hong, S. K., Shin, J., Yoo, K. W., Hibi, M., Hirano, T. et al. (2000). Analysis of upstream elements in the HuC promoter leads to the establishment of transgenic zebrafish with fluorescent neurons. *Dev. Biol.* **227**, 279-293.

Pierre, S. C., Hausler, J., Birod, K., Geisslinger, G. and Scholich, K. (2004). PAM mediates sustained inhibition of cAMP signaling by sphingosine-1-phosphate. *EMBO J.* **23**, 3031-3040.

Piper, M. and Holt, C. (2004). RNA Translation in Axons. *Annu. Rev. Cell Dev. Biol.* **20**, 505-523.

Potter, C. J., Pedraza, L. G. and Xu, T. (2002). Akt regulates growth by directly phosphorylating Tsc2. *Nat. Cell Biol.* **4**, 658-665.

Roux, P. P., Ballif, B. A., Anjum, R., Gygi, S. P. and Blenis, J. (2004). Tumor-promoting phorbol esters and activated Ras inactivate the tuberous sclerosis tumor suppressor complex via p90 ribosomal S6 kinase. *Proc. Natl. Acad. Sci. USA* **101**, 13489-13494.

Sakurai, T., Wong, E., Drescher, U., Tanaka, H. and Jay, D. G. (2002). Ephrin-A5 restricts topographically specific arborization in the chick retinotectal projection in vivo. *Proc. Natl. Acad. Sci. USA* **99**, 10795-10800.

Schaefer, A. M., Hadwiger, G. D. and Nonet, M. L. (2000). rpm-1, a conserved neuronal gene that regulates targeting and synaptogenesis in C. elegans. *Neuron* **26**, 345-356.

Schmidt, J. T., Fleming, M. R. and Leu, B. (2004). Presynaptic protein kinase C controls maturation and branch dynamics of developing retinotectal arbors: possible role in activity-driven sharpening. *J. Neurobiol.* **58**, 328-340.

Scholich, K., Pierre, S. and Patel, T. B. (2001). Protein associated with Myc (PAM) is a potent inhibitor of adenylyl cyclases. *J. Biol. Chem.* **276**, 47583-47589.

Song, H. J., Ming, G. L. and Poo, M. M. (1997). cAMP-induced switching in turning direction of nerve growth cones. *Nature* **388**, 275-279.

Sperry, R. W. (1963). Chemoaffinity in the orderly growth of nerve fiber patterns and connections. *Proc. Natl. Acad. Sci. USA* **50**, 703-710.

Tee, A. R., Anjum, R. and Blenis, J. (2003a). Inactivation of the tuberous sclerosis complex-1 and -2 gene products occurs by phosphoinositide 3-kinase/Akt-dependent and -independent phosphorylation of tuberin. *J. Biol. Chem.* **278**, 37288-37296.

Tee, A. R., Manning, B. D., Roux, P. P., Cantley, L. C. and Blenis, J. (2003b). Tuberous sclerosis complex gene products, Tuberin and Hamartin, control mTOR signaling by acting as a GTPase-activating protein complex toward Rheb. *Curr. Biol.* **13**, 1259-1268.

Trowe, T., Klostermann, S., Baier, H., Granato, M., Crawford, A. D., Grunewald, B., Hoffmann, H., Karlstrom, R. O., Meyer, S. U., Muller, B. et al. (1996). Mutations disrupting the ordering and topographic mapping of axons in the retinotectal projection of the zebrafish, Danio rerio. *Development* **123**, 439-450.

Wagle, M., Grunewald, B., Subburaju, S., Barzaghi, C., le Guyader, S., Chan, J. and Jesuthasan, S. (2004). EphrinB2a in the zebrafish retinotectal system. *J. Neurobiol.* **59**, 57-65.

Wan, H. I., DiAntonio, A., Fetter, R. D., Bergstrom, K., Strauss, R. and Goodman, C. S. (2000). Highwire regulates synaptic growth in Drosophila. *Neuron* **26**, 313-329.

Xu, L., Wei, Y., Reboul, J., Vaglio, P., Shin, T. H., Vidal, M., Elledge, S. J. and Harper, J. W. (2003a). BTB proteins are substrate-specific adaptors in an SCF-like modular ubiquitin ligase containing CUL-3. *Nature* **425**, 316-321.

Xu, L., Yang, L., Moitra, P. K., Hashimoto, K., Rallabhandi, P., Kaul, S., Meroni, G., Jensen, J. P., Weissman, A. M. and D'Arpa, P. (2003b). BTBD1 and BTBD2 colocalize to cytoplasmic bodies with the RBCC/tripartite motif protein, TRIM5delta. *Exp. Cell Res.* **288**, 84-93.

Yates, P. A., Roskies, A. L., McLaughlin, T. and O'Leary, D. D. (2001). Topographic-specific axon branching controlled by ephrin-As is the critical event in retinotectal map development. *J. Neurosci.* **21**, 8548-8563.

Zhen, M., Huang, X., Bamber, B. and Jin, Y. (2000). Regulation of presynaptic terminal organization by C. elegans RPM-1, a putative guanine nucleotide exchanger with a RING-H2 finger domain. *Neuron* **26**, 331-343.